Case Studies in Construction Materials 21 (2024) e04038

Contents lists available at ScienceDirect

Case Studies in Construction Materials

journal homepage: www.elsevier.com/locate/cscm

Ultra-thin sealing surface treatments for solar radiation screening on asphalt facing dams

Filippo Balzano [a,*], Piergiorgio Tataranni [a], Enrico Tita [b], Cesare Sangiorgi [a]

[a] Department of Civil, Chemical, Environmental and Materials Engineering, University of Bologna, Bologna, Italy
[b] CEA - Cooperativa Edile Appennino Scarl, Calderara di Reno, BO, Italy

ARTICLE INFO

Keywords:
Asphalt dams
Sealing membranes
Colorimetry analysis
Solar irradiance
Lightweight aggregates

ABSTRACT

Bituminous materials are widely used in a large range of hydraulic applications due their excellent waterproofing properties. More than 300 asphalt facing reservoirs were built in the last century, presenting higher mechanical and hydraulic performance when compared with other facing alternatives, such as cement concrete or steel membranes. On the other hand, the dark colour of bitumen may lead to high temperatures inside asphalt paved system, affecting long term ageing of binder and jeopardizing the quality of the impervious layer. Recently, multifunctional ultra-thin surface treatments are becoming an alternative to demolition-reconstruction of the impervious layer, significantly abating the quantity of energy and raw materials required for maintenance. High-reflective surface treatments may represent also an effective solution to reduce the temperature of asphalt layers, extending the service life of the dam embankment and reducing the need of maintenance. In fact, there is a lack of literature concerning the assessment of thermal impact on asphalt dams. In the light of above, a number of different combinations of sealing surface treatments were investigated in this study. An *ad hoc* testing equipment and procedure were designed to perform an artificial solar irradiance test. A complete colorimetry analysis was performed and the outcomes were compared with temperature data, making use of a thermal camera and of embedded sensors for surface and base temperature measurements, respectively. Major results and their relationships have been commented in-depth along with proposed further research activities.

1. Introduction

1.1. Asphalt facing dams

Waterproofing properties of bituminous materials were widely recognised since ancient times [1]. The oldest know application of a primitive bituminous concrete as impervious membrane can be observed in the dam of Assur (Mesopotamia), which dates back to 1300 B.C. [2], giving testimony of the antiquity of this concept. Therefore, bitumen was used in a large range of hydraulic applications including canal linings, coastal constructions and dams, in recent centuries [3]. As for the modern times, more than 300 asphalt facing reservoirs were built since 1920s [4], reaching heights sometimes above 150 m [5] and slopes up to 1:1.5 in the upstream wall [6]. The

* Corresponding author.
E-mail addresses: filippo.balzano2@unibo.it (F. Balzano), piergiorg.tataranni2@unibo.it (P. Tataranni), e.tita@cea-coop.it (E. Tita), cesare.sangiorgi4@unibo.it (C. Sangiorgi).

https://doi.org/10.1016/j.cscm.2024.e04038
Received 2 September 2024; Received in revised form 15 October 2024; Accepted 25 November 2024
Available online 27 November 2024

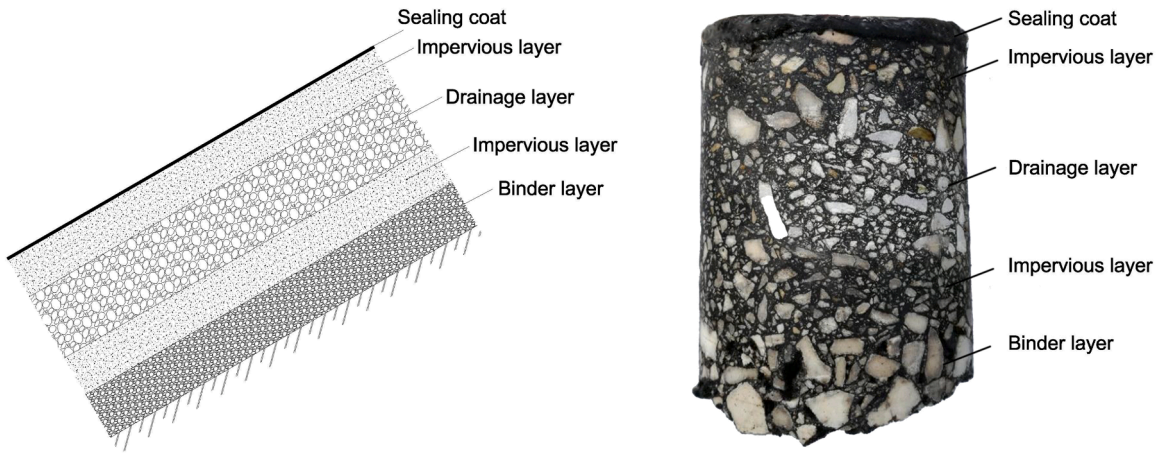

Fig. 1. Typical cross-section and core of an asphalt concrete impervious membrane.

Fig. 2. Common failures on asphalt dams: **a)** Cracking failure (Los Angeles, USA) [21]; **b)** Slippage failure (Paduli, Italy); **c)** Blistering failure (Zhangewan, China) [10].

application of asphalt concrete as impervious layer generally increases the safety factor against seepage, when compared with other facing alternatives such as cement concrete or steel membranes [7]. Moreover, other advantages include lower construction and maintenance costs, rapid realization times and higher resistance against erosion under the action of water flowing. In addition, asphalt can be considered physiologically harmless and does not preclude its use in reservoirs containing potable and irrigation waters [3]. Commonly, the impervious asphalt concrete is layered as a double lining membrane, as described in Fig. 1 [6]. A transition layer of binder mixture (usually 4–10 cm thick) is initially laid down to level the irregularities of the embankment and to serve as a base layer for the bituminous system. Afterward, a first impervious layer of dense asphalt concrete (6–8 cm) is laid. A minimum void content of 2–3 % is guaranteed in any case, to prevent micro-cracking due to thermal deformations during the service life of the mixture [8], as for void contents below 3 % the permeability coefficient of asphalt is less than 10^{-8} cm/s and the layer can be considered impermeable [9]. A drainage layer, consisting in a porous bituminous concrete mixture (5–15 cm, void content of 16–20 % [10]) is then placed and subsequently covered with the second impervious layer. At the end of the construction process, a sealing coat of bituminous emulsion or hot bituminous mastic (1–2 mm) is spread over the surface to serve as a weathering protection barrier [6]. Alike the construction of road pavements, the application of a bituminous emulsion tack coat between the layers is decisive to avoid any slippage cracking at the interfaces [11].

On one hand, many researches proved that the impervious layered asphalt system, which normally has a total thickness ranging between 20 and 45 cm, can successfully withstand common operating water column pressures up to 200 m [8] without any considerable hydraulic fracturing effect [12]. On the other hand, foundation differential settlements may occur, causing a tensile stain status that, in specific conditions, may result in serious cracking when the material is not flexible enough to accommodate the movements of the substrate [13]. Furthermore, bitumen is a viscoelastic and thermoplastic material [8] and its properties change considerably with temperature. For this reason, different types of distresses may occur due seasonal climatic fluctuations, which in some case may lead to temperatures ranging from −30 °C to 80 °C in the external thickness of the membrane [3,10,14]. Thermal stresses are typically relieved by asphalt concretes with an appropriate dimensioning and composition, but temperature oscillations, aging effects, swashing of water and solar radiations strongly affect the long-term ageing process of unprotected surfaces [1]. In this regard, freezing-thawing conditions may induce damages to the exposed layers, resulting in diffuse cracking that may jeopardize the waterproofing effect of the membrane [15]. In addition, upstream surface is constantly exposed to ultraviolet radiations [16], which cause evaporation of bitumen's volatiles accelerating its ageing process [17,18], hardening the bituminous concrete and resulting in a brittle and cracking sensitive behaviour (Fig. 2**a**) [8,19]. Solar radiation exposure during the hot season, considering the low reflectance of bituminous

Fig. 3. a) High pressure cleaning and resealing of the embankment surface; **b)** Application of an in-situ sealing membrane; **c)** Multi-layered in-situ sealing membrane with aggregate finishing.

faced surfaces, which generally is not above 5–10 % [20], results into very high temperatures inside the membrane and this may lead, especially when high slopes are required, to relative interlayer slippage failures. (Fig. 2**b**). Moreover, when temperatures inside the membrane rise above 55–60 °C, the water enclosed between the impervious layers tends to reach vapour pressure, leading to local blistering phenomena that can result in serious deformations and cracking of the outer face (Fig. 2**c**)[10].

In the light of above and considering the long service life required for dams, typically over 100 years [22], an effective maintenance strategy is essential to anticipate degradation and to adequately repair damaged layers. State of the art of asphalt dams' maintenance is moving away from demolition-reconstruction of the impervious layer, since milling and repaving operations involve enormous quantities of energy and raw materials. Moreover, slope conditions require high-specialized operators and equipment, which drastically increase the costs of the intervention [23]. For these reasons, spot repairing and diffused resealing treatments are often preferred. Limited major cracks are generally treated with injections of sealing mastic, which is typically bitumen-based and cold applied [24]. For diffused degradation, periodically restoring the sealing coat is often required. Outer centimetres of the asphalt system are removed with high-pressure water (250 MPa) and visible cracks are resealed with mastic (Fig. 3**a**). A new sealing coat is then laid spraying bituminous emulsion or hot bitumen by using nozzles [23]. Alternatively, prefabricated bituminous membranes [14], often containing glass fibres or polymeric grids, may be applied [25].

In recent years, many contracting authorities are also encouraging the use of multifunctional surfacing treatments as replacement and/or integration of the traditional sealing coating techniques, in order to improve the performance of the embankment and aiming to extend its durability. Depending on the case, these may consist in the application of particular modified bituminous emulsion (cold) [11] or bitumen (hot), sealing mastic (hot) [24], non-bituminous coating (hot or cold), painting (cold) up to represent properly designed surfacing treatments (cold or hot). Regardless to mechanical performance, more sophisticated surfacing treatments also allow to include in this type of applications environmental and landscaping impact aspects. Indeed, dams are large constructions that can dominate and completely alter local landscapes [26], especially when dark coloured asphalt surfaces are visible over the embankment in low-water level periods. Thus, to mitigate the visual impact of this structures on the surrounding landscape, specific coating techniques, which generally consist in a particular colouration or surface finishing, are often applied [27].

1.2. Surfacing treatments in asphalt dams

Surfacing applications may be very different, but frequently are performed using machineries borrowed from the road paving industry that are converted to operate in high-slopes conditions. Commonly, they include a paver that moves upwards on the embankment by means of a winch, a system of nozzles and a spreader to allow the simultaneous laying of binder, typically hot bitumen, and aggregates, when required (Fig. 3**b**). The viscosity of bitumen ensures the immediate adhesion of aggregates in a single granular layer, generally not requiring mechanical compaction (Fig. 3**c**). Depending on the case, multiple overlapped coats of binder and aggregates, which may vary in type, gradation and dosage, may be applied to form an ultra-thin impervious membrane.

The purposes of these interventions are often targeted on the specific design problems and they are strictly related to the position of the embankment (orientation, latitude and altitude), to its geometry (height and slope), water pressure and solar exposure. As for the latter, the dark colour of bitumen contributes to amplify the quantity of solar radiation absorbed by the surface, thus increasing the temperature of asphalt layers [28]. There is a lack of literature concerning the assessment of thermal impact on asphalt dams.

1.3. Thermal effects of solar radiations on asphalt dams

From a rheological standpoint, prolonged high temperatures expose asphalt to several damages including rutting, slippage, bleeding and, in general, thermos-oxidative ageing, which reflect in a less-durable and less-performant layer [29,30]. Facing surface temperature is influenced by a number of factors such as solar irradiance, inter-molecular heat transfer, air temperature, wind's velocity and direction [15]. Irradiance is defined as the radiant flux incident on a surface per unit area and, according to ISO 9845–1 and many other studies, may be globally assumed approximately of 800–1400 W/m^2 [31]. Ozone in the stratosphere absorbs almost every radiant energy having the wavelength below 295 nanometres [32], so that the solar spectrum that reaches Earth's ground is contained within 295 and 2450 nm [33]. Wavelengths included in the range 380–780 nm (42–43 % of total spectrum) form visible light (VIS) [34] and can be appreciated by human eye. Shorter wavelengths (295–380 nm) are considered ultraviolet (UV) and represent 3–5 % of

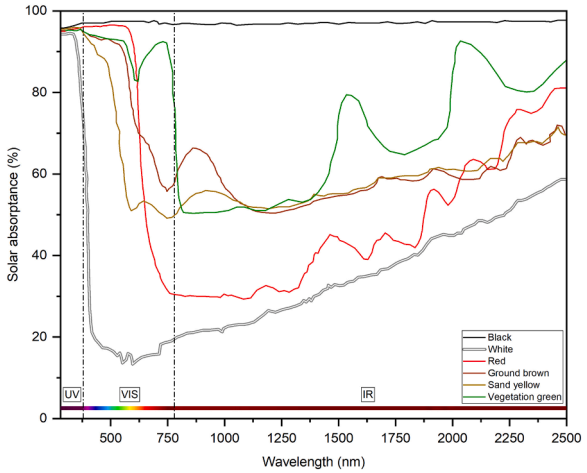

Fig. 4. Solar absorptance on different coloured opaque surfaces [42–45].

solar light spectrum on Earth [32]. In the end, short frequency waves (780–2450 nm) identify the infrared (IR) portion and consist in the remaining 52–55 % of solar spectrum. Distinguishing between these sub-regions is essential, since each portion of light is associated to different phenomena and effects on the dam surface. Although thermal contribute of UV light is negligible [35], its short wavelengths (high energy) can destroy molecular structure of material [36], playing a major role in accelerating the photo-oxidation ageing of the binder [37] and resulting in a general performance degradation of the layer. On the other hand, photons of VIS and, especially, IR light move at wavelengths that can pass through the molecules and in part being absorbed, leading to a gain of energy that generates charge-acceleration, resulting in an increasing of matter temperature [38]. The light portion that is not absorbed by surface is reflected as filtered light and it is perceived from the photoreceptor (e.g. human eye) as object's colour [39]. Solar reflectance of a surface is the percentage of incident sunlight that is reflected [40]. In low-solar reflective surfaces the difference of temperature between the surface and ambient air may sometimes reach 50 °C [41,42]. Opaque surfaces absorb light differently in the three spectrum regions [42,43] and, as shown in Fig. 4, the highest difference in solar absorbance between black and coloured surfaces lies in the IR region [43].

High-reflective surface treatments may represent an effective solution to reduce the temperature of asphalt layers of the embankment, extending its service life and reducing the need of maintenance. Colour is not a physical property of the surface but rather a receptor perception enabled by light, so adopting an objective evaluating method is essential. In this regard, colorimetry provides different options for quantitative measurement of colours and their numerical elaboration [46–48]. In particular, CIELAB colour space is universally accepted as colorimetric reference system in scientific applications. Unlike other systems (e.g. RBG, CMYK), it is unambiguous, absolute and device independent [49], since it is directly based on light stimulus values in a trichromatic reference system [39], expressed as the non-linear coordinates L*, a* and b* according to EN ISO/CIE 11664–4 [50].

L* is the luminance of the stimulus, which represents the lightness, and ranges from 0 (pure black) to 100 (pure white). a* axis represents the greenness (-a*) or the redness (+a*), while b* axis indicates the yellowness (-b*) or the blueness (+b*) of colours. When numerical values are assigned to each coordinate, any colour can be univocally located in a three-dimensional colour space, allowing its description and mathematical elaboration [51].

An unambiguous colour description allows a methodical classification of dark and clear surfaces, enabling the definition of landscape-compatible tones to include in the mitigation process of the embankment, which may be achieved using a surface treatment.

In the light of above, this study aimed to test traditional and innovative solutions as possible surface treatments for asphalt dams. Main importance was given to solar radiations screening properties of the impervious system, with the purpose of improving the short-term thermal performance of the state-of-the-art sealing coats. Effectiveness of the intervention was evaluated in terms of surface temperature and asphalt support temperature, measured with advanced equipment. In addition, the reduction of visual impact of the asphalt faced surfaces was investigated, proposing landscape compatible coloured sealing coats and using innovative ultra-thin layered sealing membranes, in different configurations. A complete colorimetric analysis of the external surfaces was conducted and the outcomes of thermal tests were correlated with the chromaticity parameters, and later discussed.

2. Materials and methods

2.1. Materials

In order to extend the effectiveness of this study, a large number of possible surface treatments for asphalt dams were lab-prepared and tested, including conventional (control) and novel materials as listed hereafter: two hot polymer-modified bitumen and 5 alternative "non-black" sealing surfacing; 25 different monogranular membranes (consisting in a single layer of aggregates between two coats of binder); 8 double-layered membranes, with an additional finishing coating of fine aggregates. All 40 combinations presented

Table 1
Group classification of the tested surface treatments.

Configuration	Description	Thickness [mm]	Weight [kg/m^2]
Sealing coat	Binder coating	1.9 – 2.1	2.0 – 2.5
Single-layered membrane	Monogranular membrane with binder finishing	8.8 – 12.0	8.2 – 13.0
Double-layered membrane	Monogranular membrane with aggregates finishing	15.2 – 18.2	9.8 – 23.7

Table 2
Volumetric and mechanical properties of virgin aggregates.

Test	Unit	Basalt	Limestone	Pale limestone
Notation	-	B	C	W
Particle density (EN 1097–6)	g/cm^3	2.713	2.658	2.674
Resistance to fragmentation LA (EN 1097–2)	%	20	20	21
Resistance to polishing (EN 1097–8)	PSV	50	44	42

Table 3
Volumetric and mechanical properties of lightweight aggregates.

Test	Unit	LECA-P	LECA-S
Notation	-	LP	LS
Loose bulk density (EN 1097–3)	g/cm^3	0.425	0.624
Particle density (EN 1097–6)	g/cm^3	0.763	1.254
Percentage of voids (EN 1097–3)	%	44.34	50.24
Water content (EN 1097–5)	%	0.95	9.40
Crushing resistance (EN 13055–1)	N/mm^2	3.198	6.155
Water absorption after 24 h (EN 1097–6)	%	5	18
Freezing and thawing resistance (EN 13055–1)	%	0.86	0.71

Table 4
Properties of binders.

Notation	Description	Penetration [dmm]	Softening point [°C]
PmB_1	PmB (SBS+EVA)	26	99
PmB_2	PmB (SBS)	51	82
TB	Polyolefin-based synthetic binder	55	75

in this study, which can be grouped according Table 1, were prior tested for their use in terms of waterproofing capacity, adhesion to the support layer and thermal stability.

2.2. Aggregates

An accurate selection of the type, size and colour of aggregates was required for this study. Two natural virgin aggregates (basalt and limestone), provided by a local quarry were selected due their large use in current asphalt dams' maintenance. A second type of limestone with a high-content of calcium carbonate, provided by a quarry in central Italy was tested for its light-colour properties and its wide use in local highly-reflective urban pavements [52]. Table 2 lists the main volumetric and mechanical properties of the adopted virgin aggregates.

Moreover, this study proposes the use of Lightweight Expanded Clay Aggregates (LECA), characterized by high porosity and low density [53], as an innovative solution to reduce the total weight of the membrane and to avoid its relative slippage in steep conditions. LECA is a widely available and standardized civil engineering material [54], produced by firing raw clay in a rotary kiln. The gases expand the clay, generating granules with a strong shell and a porous inner core [55]. In addition, its clay composition confers to LECA a natural soil colour, which makes it suitable for mitigation in non-urbanized contexts. Two different types of commercially available LECAs were selected. LECA-S presents a higher soundness and was used a structural aggregate in the first layer of the membrane. On the contrary, LECA-P is lighter and less resistant to mechanical actions, but it is manufactured including a hydrophobic treatment that makes it less water sensitive, and so it was selected as finishing aggregate when required. Table 3 collects the main volumetric and mechanical properties of LECA, according to general lightweight aggregates requirements.

2.3. Binders

Three different binders, which properties are shown in Table 4, were tested. Two commercial polymer-modified bitumen (PmB),

Table 5
Description of pigments.

Notation	Colour	Main component	Supplied as
w	White	Titanium dioxide (Ti_2O)	Pellets
r	Red	Iron oxide (FeO)	Pellets
g	Green	Chromium Oxide (Cr_2O_3)	Powder

Table 6
Summary table of the tested surface treatments.

Notation	Aggregate	N°	Description
DL | PmB_1_	L, C, B, W	8	Double-Layered membrane presenting two coats of PmB_1 and two coats of L, C, B and W aggregates
DL | PmB_2_	L, C, B, W	8	Double-Layered membrane presenting two coats of PmB_2 and two coats of L, C, B and W aggregates
SL | PmB_1_	L, C, B, W	8	Single-Layered membrane presenting two coats of PmB_1 and one coat of L, C, B and W aggregates
SL | PmB_2_	L, C, B, W	8	Single-Layered membrane presenting two coats of PmB_2 and one coat of L, C, B and W aggregates
SL | TB_	L, C, B, W	8	Single-Layered membrane presenting two coats of TB and one coat of L, C, B and W aggregates
SL | PmB_1_r_	L, C, B, W	10	Single-Layered membrane presenting two coats of PmB_1, r pigments and one coat of L, C, B and W aggregates
SL | PmB_1_w_	L, C, B, W	10	Single-Layered membrane presenting two coats of PmB_1, w pigments and one coat of L, C, B and W aggregates
SL | TB_g_	L, C, B, W	8	Single-Layered membrane presenting two coats of TB, g pigments and one coat of L, C, B and W aggregates
PmB_1	-	2	Sealing coat of PmB_1 binder
PmB_2	-	2	Sealing coat of PmB_2 binder
TB	-	2	Sealing coat of TB binder
PmB_1_r	-	2	Sealing coat of PmB_1 binder with r pigments
PmB_1_w	-	2	Sealing coat of PmB_1 binder with w pigments
TB_g	-	2	Sealing coat of TB binder with g pigments

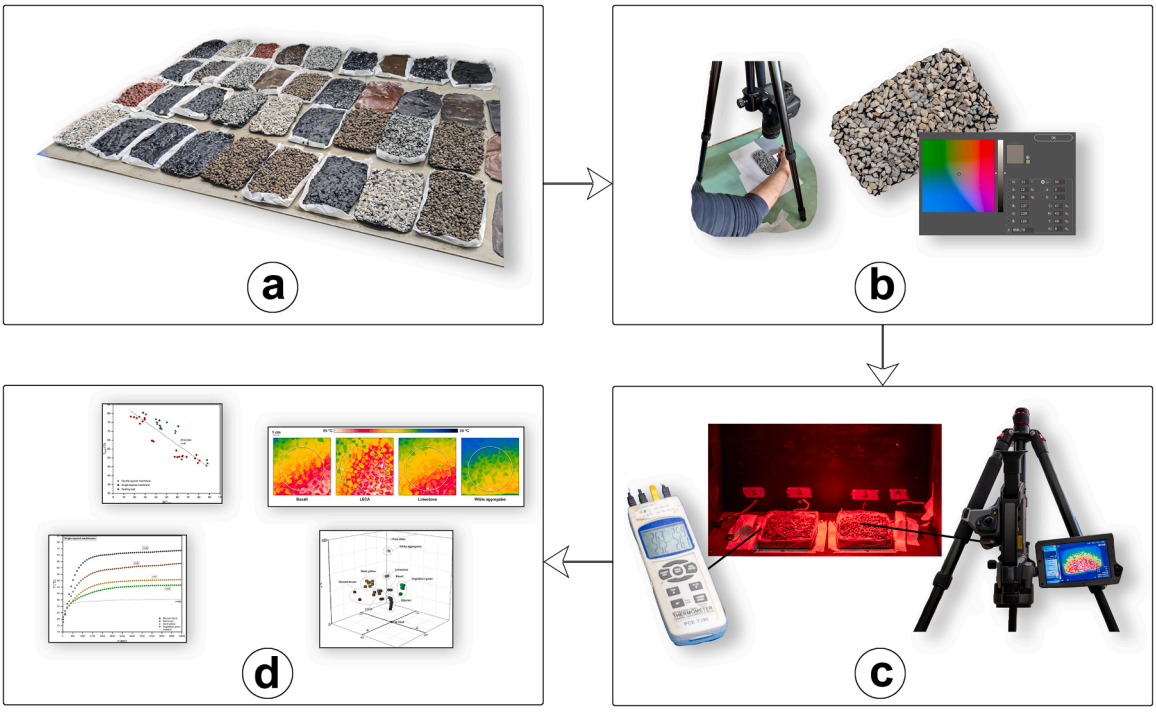

Fig. 5. Flow chart of the experimental methodology: a) samples' preparation; b) colorimetry analysis; c) artificial solar irradiance test; d) analysis of results.

which respectively contain elastomers (SBS) and elastomers + plastomers (SBS + EVA), were selected due their common use in local asphalt dams' sealing layers maintenance. In addition, a commercially available polyolefin-based synthetic transparent binder manufactured by mixing polymers, resins and oils [52], was proposed for its low-visual impact road applications.

Moreover, commercial pigments commonly used in coloured asphalt pavements were eventually added to binders, in different formulations, in order to obtain low-visual impact coloured finishing compatible with high-reflective properties. All the selected pigments, described in Table 5, were certified for their environmental compatibility.

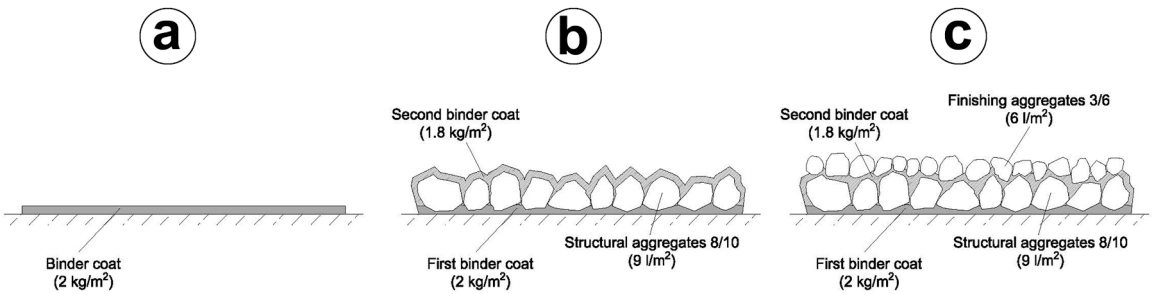

Fig. 6. Cross section of the three different surface treatments: a) sealing coat; b) single-layered membrane; c) double-layered membrane.

Pigments were directly added to the hot binder (wet modification process [8]) and mixed using a laboratory high-shear mixer at 4000 RPM for 10–30 minutes, following the manufacturer suggestions. The percentage of pigments was selected in order to obtain chromaticity coordinates within nature compatible colour ranges. Red and white pigments were added to black bitumen in different percentage to obtain soil brown and sand yellow colours. Green pigments were combined with transparent binder in order to achieve vegetation green colour.

The following Table 6 provides a summary of the tested alternatives, referring to the notations above introduced.

3. Methods

Representative samples of each surface treatment were manufactured in the laboratory. Surfaces were photographed with a specific procedure and a complete colorimetry analysis was performed. Samples were subjected to a cycle of artificial solar irradiance, making use of a near-infrared thermal lamp that replicates high-irradiance solar conditions in hot season. A system of thermocouples was placed at the base of the membranes to record the temperature of their support (asphalt dam impervious layers) in continuous. Moreover, temperature of the external surface of samples was measured during the test with a high-resolution thermal camera (FLIR Systems P620). Results obtained for surface treatments within different groups and with different materials were compared and discussed. Eventually, the outcomes of colorimetry analysis were correlated with the thermal properties of the membranes. The flow chart in Fig. 5 depicts the above-described main phases of the study.

3.1. Samples' preparation

In order to reproduce the in-situ composition of the tested membranes in a reduced laboratory scale, a rigorous procedure was followed. Dosage of materials, their distribution and laying conditions were taken from real applications and adapted on the specific case to achieve the same thickness and composition of real membranes. A first film of binder, which is the one in contact with the impervious asphalt layer and has to play the role of sealing coat, had a thickness of 1.9–2.0 mm (e.g. 2.0 kg/m^2 of PmB), while the second binder coating was 1.7–1.8 mm thick (e.g. 1.8 kg/m^2 of PmB). Structural aggregates layer consisted in a monogranular coating of 8/10 mm size aggregates, distributed with a dosage of 9.0 l/m^2. Eventually, finishing aggregates with a dosage of 6.0 l/m^2 and a 3/6 mm size were applied after the second laying of binder, resulting in the double-layered membrane configuration, as shown in Fig. 6.

Samples were manufactured in rectangular casting moulds (10.5 ×17.5 cm), pre-coated with laboratory paper. Binder was heated in a thermostatic oven at sampling temperature, according to EN 1427. The amount of material required to obtain the design thickness of the first and the second layer of binder was poured in two different moulds on a high-precision laboratory scale, and placed in the oven for 10–15 minutes until levelled films were obtained. The first coating film was placed on a flat surface and immediately covered with the structural aggregates. In order to replicate the action of the in-situ spreader box machine, aggregates were poured through a 12 mm sieve, which size is larger than the maximum diameter of aggregates, to ensure a randomised distribution of particles and to prevent the segregation of heavier ones. Hot temperature of binder promoted the adhesion of aggregates without any compaction effort. The mould was allowed to reach room temperature and then the excess aggregates, which were not in direct contact with the binder film, were carefully removed. The second film was removed from the oven and left to reach temperature room inside the mould. Afterward, it was detached from the parchment paper and laid on top of the structural aggregates layer. The system was put in the oven for 10–15 minutes to allow the melting of binder and the adhesion between the elements. Eventually, the finishing aggregates were poured on the hot binder through an 8 mm sieve where a double-layered configuration was required. At least two replicates for each configuration were produced.

3.2. Colorimetry analysis

Top surface of each sample underwent a process for the determination of chromaticity coordinates and a series of colorimetry parameters. It was photographed by means a professional 30.4 MP full frame DSLR camera and a prime 100 mm macro-lens, in controlled studio conditions. Exposure was measured with a 150.000-pixel RGB-IR metering sensor, having 252 evaluative zones, and adjusted to a EV 0 exposure value. Temperature of light was corrected by using a set of PVC-coated professional calibrating cards,

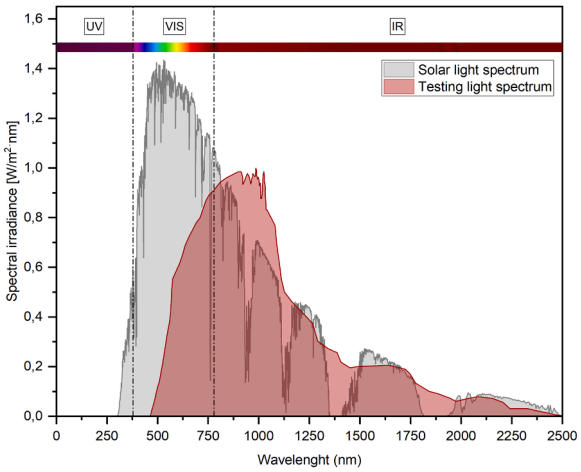

Fig. 7. Spectral power distribution of solar light and testing conditions [56].

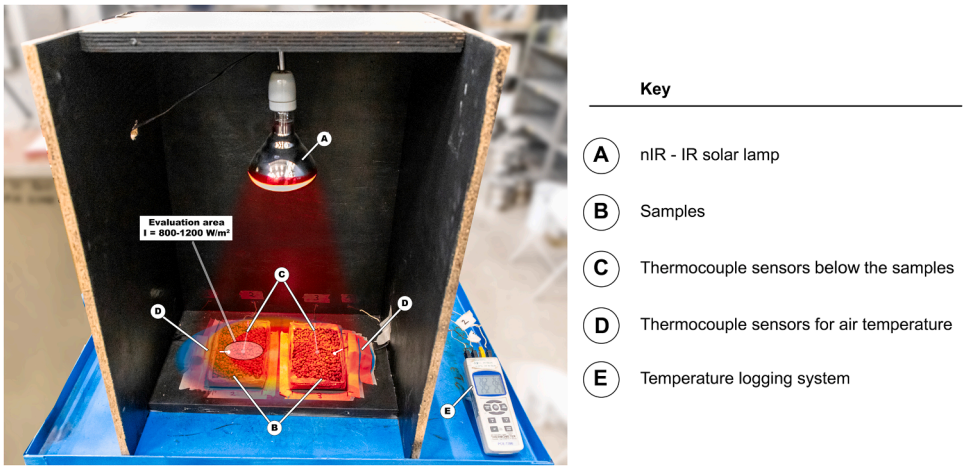

Fig. 8. Artificial irradiance testing setup.

setting white balance manually referring to the 18 % neutral grey card. Finally, a circular polarizer filter, having a 28 layers 0.2 % ultra-low reflectivity nano-coating, was used to reduce the light effects on reflective surfaces. Photographs were analysed using the proprietary software Adobe Photoshop CC 2023 v.24.5 and the chromaticity coordinates L*, a* and b* in the CIELAB colour space were extracted, expressed as the medium values evaluated in the central area of the specimen (radius 40 mm). Chromaticity coordinates were used to uniquely locate each surface colour in a three-dimensional space system and to provide its mathematical elaboration. In particular, the position of the point in the CIELAB colour space was evaluated by means of the colour difference ΔE^*_{Lab}, defined as the Euclidean norm of position vector to a reference point [40]. Referring to the origin of the CIELAB space with coordinates (0, 0, 0), ΔE^*_{Lab} expresses the distance between a colour and pure black, which is the less light reflective possible colour. ΔE^*_{Lab} can quantify the magnitude of the colour difference, but does not necessarily indicate the direction and the orientation of the vector. In the light of above, Hue and Chroma parameters were also calculated according to EN ISO/CIE 11664–4, as follows:

$$\Delta E^*_{Lab} = \sqrt{\Delta L^{*2} + \Delta a^{*2} + \Delta b^{*2}}$$

$$C^*_{ab} = \sqrt{a^{*2} + b^{*2}}$$

$$h_{ab} = \arctan\left(\frac{b^*}{a^*}\right)$$

where:

– L*, a*, b*→are the coordinates in CIELAB colour space;

Fig. 9. Surface appearance of sealing treatments: **(top)** double-layered membranes with different finishing aggregates; **(centre)** single-layered membranes with different finishing binder; **(bottom)** sealing coats.

- ΔE^*_{Lab}→is colour difference in CIELAB colour space;
- C^*_{ab}→is Chroma in CIELAB colour space;
- h_{ab}→is Hue in CIELAB colour space.

Hue and Chroma are lightness-independent polar coordinates of chromaticity. Hue is expressed as the angular value that unambiguously indicates redness (0°), yellowness (90°), greenness (180°) or blueness (270°) of colours in a classified continuous colour wheel scale, according to dominant wavelengths of light reflected. Hue is conventionally ordered following the colour pattern observed when white light is passed through a glass prism. Chroma is the radius value in the polar coordinates system and describes the degree of purity of a colour in relation with neutral grey. Chroma expresses the colourfulness of a hue and allows to distinguish between achromatic and saturated colours. All the above-mentioned colorimetry properties were detected on the samples before testing and are presented in the following sections.

3.3. Solar irradiance test

In order to reproduce high-irradiance solar conditions in a laboratory scale, an *ad hoc* testing equipment and procedure were designed. A 250 W near-infrared/infrared solar lamp was selected (Philips BR125). As shown in Fig. 7, the equipment was calibrated to

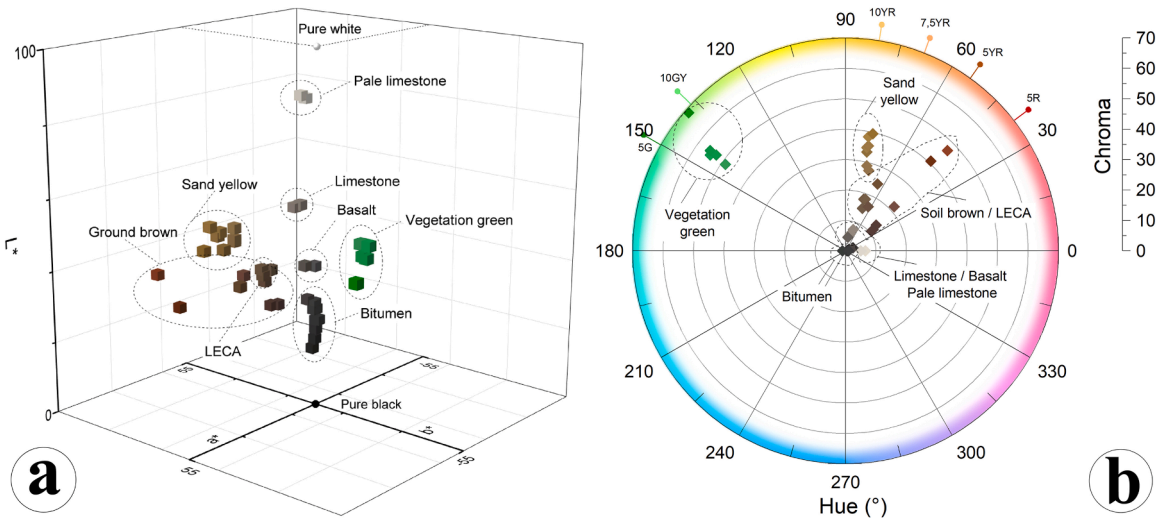

Fig. 10. a) chromaticity coordinates in the three-dimensional CIELAB colour space; **b)** Hue and Chroma in a polar coordinates' representation.

replicate natural solar irradiance in the nIR/IR spectrum, since the effect of light frequencies out of this range was considered negligible on temperature.

The lamp was located in a black painted environment, at the distance of 40 cm from the tested samples, and directly oriented. The setup, which is illustrated in Fig. 8, allowed to test two identical samples simultaneously and to express results as their average values. Samples were placed in isolated vessels and their position inside the box was calibrated to obtain a measured value of irradiance in the central area of the surfaces ranging from 800 to 1200 W/m^2. Thermocouple sensors were installed in the central area below each sample. Another couple of sensors was positioned approximately 0.5 cm over on the top of irradiated surfaces, to provide ambient temperature measurement. Positioning of the equipment was led by the will of excluding from the investigation points belonging to the border region of the specimen, which may be influenced by exposure differences and other factors.

Samples were conditioned at 20 °C in a thermostatic climatic chamber for at least 8 hours before testing. High-irradiance conditions were kept constant for 180 minutes, in order to lead to an accelerated steady-state temperature equilibrium [41,57]. A high-resolution thermal-camera was used at regular intervals of 60 minutes to record the external surface temperature during the test. Measured surface temperatures have been compared with those of Federal Highway Administration (FHWA) Superpave Binder selection guidelines and many other studies [15,33,58–60] to ensure an analogy with highest annual pavement temperatures registered in the temperate belt, which includes large part of Europe, United States and Asia, assessing the reliability of the selected artificial solar irradiance conditions before any data elaboration.

4. Analysis of results

4.1. Results of colorimetry analysis

As introduced in previous sections, a series of materials (aggregates, binders, pigments) were combined to obtain a wide assortment of sealing surface treatments, which can be exemplified as shown in Fig. 9, keeping constant dosages, gradation of aggregates and laying condition in order to prevent differences through the thickness of membranes and ensure the comparability of results within the same treatment class.

All samples underwent to a complete colorimetry analysis prior testing, as described in previous sections. Chromaticity coordinates in the three-dimensional CIELAB colour space were collected and represented in Fig. 10**a**.

Bitumen coated surfaces presented a L* parameter ranging between 17 and 30, which correspond to dark colours. Coloured binders generally increased the lightness of surfaces: L* for soil brown colourations ranged between 30 and 41 (+12 % on average), while lightness of sand yellow and vegetation green was 50–57 (+30 % on average) and 55–60 (+34 % on average) respectively. As expected, double-layered membranes finished with LECA presented a brownish tonality and a L* parameter falling in the soil colours range (L* = 41). Hence, the use of natural aggregates as finishing material allows increasing the lightness of the dam surface of +17 % (L* = 40–41), +34 % (L* = 57–58) and +64 % (L* = 87–88) for basalt, limestone and pale limestone, respectively.

In addition, as shown in Fig. 10**b**, Hue and Chroma values were calculated from the lightness-independent parameters a* and b*. Bitumen coated and natural aggregates finished surfaces resulted nearly achromatic, centring in the area with null values of chroma in a polar coordinates representation. On the contrary, soil-coloured surfaces, as well as those finished with LECA, hued between 37°-70°, falling within the range 10 R – 7.5YR in Munsell Colour Chart (MCC) soil classification [61], which reflects some of the most common natural soil hues [51,62]. Sand-coloured surfaces hued between 73° and 78°, corresponding to 7.5YR – 10YR in MCC soil classification. In the end, green-coloured membranes presented a hue between 138° and 144°, within the range 10GY – 5 G in MCC plant

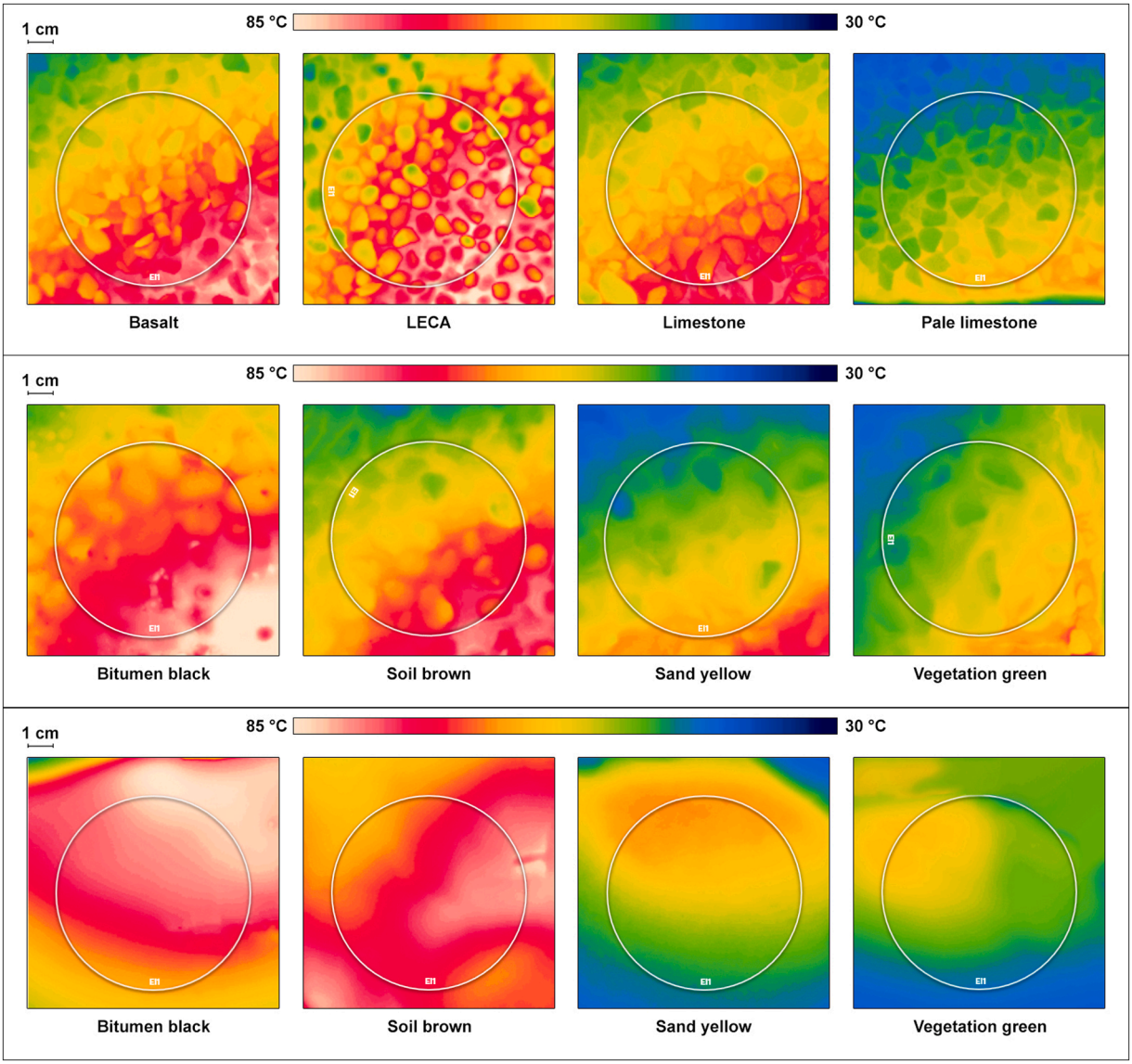

Fig. 11. Thermophotos of specimen after the irradiance test: **(top)** double-layered membranes; **(centre)** single-layered membranes; **(bottom)** sealing coatings.

classification [63], which can be reasonably assumed compatible with fresh grass and vegetation [64].

4.2. Results of surface temperature analysis

As already mentioned, colors are perceived as an effect of the filtered light reflected, and consequently absorbed, by surfaces at different frequencies. Superficial temperature (T_{SUP}) is strongly connected with the quantity and the quality of solar radiations that can pass through surface (e.g. exposure to 1000 W/m^2 of UV light may produce different effects than 1000 W/m^2 of IR light) and, as can be observed in Fig. 11, is colour-dependent.

Lighter surfaces presented lower temperature after testing, resulting in an acceptable correlation (R^2 higher than 0.68) when directly comparing L* and T_{SUP} (Fig. 12**a**), similarly to other studies [65].

Hue and Chroma also play a role in light-absorptance, since the correlation index R^2 increases to 0.77 by comparing T_{SUP} with the position vector ΔE^*_{Lab} (Fig. 12**b**), referred to pure black coordinates (0,0,0). Although Euclidean norm may not be adequate to interpret the behaviour of darker colours, it can be generally observed how the surface temperature decreases by increasing the distance between the tested colour and pure black, which is the less reflective colour possible (100 % of light absorbed). Average surface temperature differences, compared with those of black bitumen coated surfaces, are reported in Fig. 13.

Results of surface temperature reduction for aggregates- and coloured binders-finished membranes have been found compatible

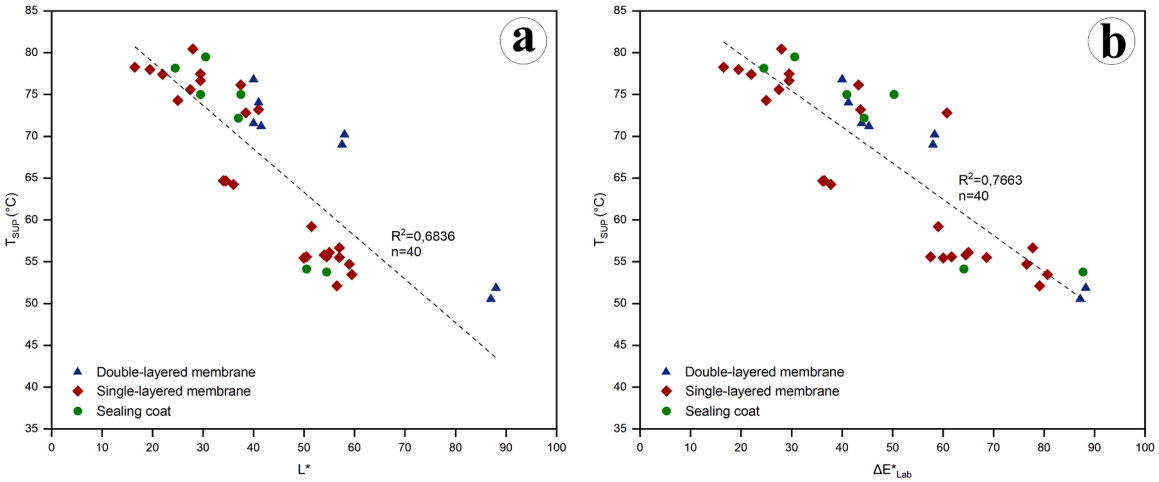

Fig. 12. **a)** relationship between L* and T_{SUP} after solar irradiance test; **b)** relationship between ΔE^*_{Lab} and T_{SUP} after solar irradiance test.

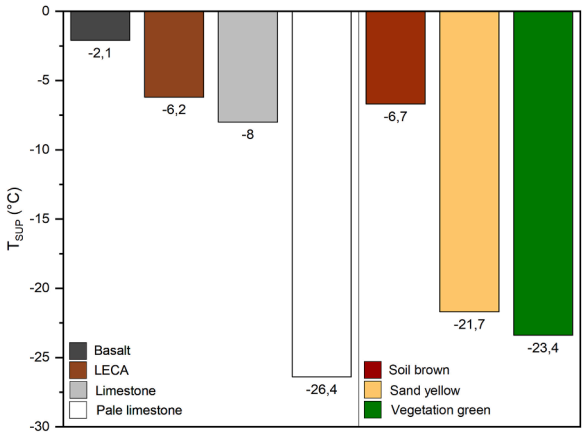

Fig. 13. Surface temperature differences referred to bitumen coated sealing treatments.

with those obtained in other studies on pigmented and clear asphalt pavements for Urban Heat Island reduction purposes [60,66]. Remarkable results in surface temperature reduction have been obtained for green-hued membranes, due their high-reflectivity in the nIR-IR region of light spectrum [44]. In fact, green colour has been selected by plants in the course of evolution to reflect unhealthy IR waves and absorb light at lower frequencies to promote photosynthesis [67,68]. It is noteworthy to highlight how thermophotos confirmed a continuous radial exposure inside the selected evaluation area, limiting border effects to points belonging to the region outside the central part of the specimen.

4.3. Results of base temperature analysis

Overall thermal screening effect of sealing surface treatments was then analysed by comparing temperature data of sensors at the base of samples, which also depends on thickness (Table 1) and on the materials used. As can be observed in the following Fig. 14, base temperature (T_{BAS}) became nearly-asymptotic (Steady-State Temperature) earlier for sealing coats (after 21 minutes on average), and than for single-layered (41 minutes on average) or for double-layered membranes (55 minutes on average), as effect of thermal transmittance delay through the thickness. Since the difference between surface temperature and base temperature for sealing coats was less than 1 °C on average, it can be concluded that heat was entirely transmitted through their thickness. However, as shown in Fig. 14**a**, pigmentation of sealing coats resulted in a mean difference of 14.8 °C between black bitumen and light-coloured binders, reflecting the results of surface temperature analysis (Fig. 14**b**). On the other hand, single-layered membranes reduced the embankment temperature of 5.3 °C on average, when compared with the corresponding sealing coat alternative. Effect of pigmentation resulted in a total decrease of temperature of 10.1 °C, 22.8 °C and 27.1 °C for soil brown, sand yellow and vegetation green treatments, respectively, when compared with black membranes (Fig. 14**c**). Result of temperature diffusion through the thickness have been found compatible with those obtained by other researchers [15,69]. Finally, double-layered membranes provided a base

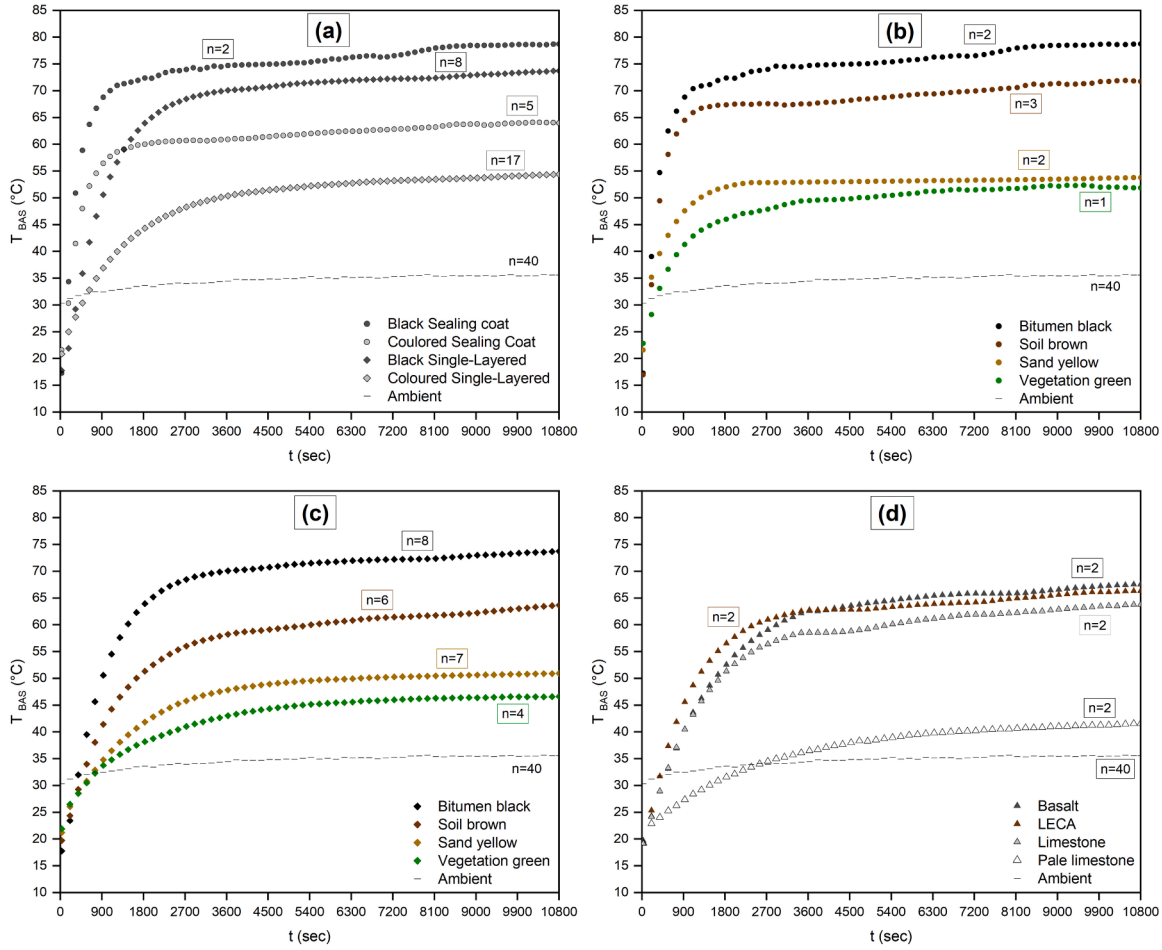

Fig. 14. Results of Base Temperature read during artificial solar irradiation test: **a)** Comparison between black and coloured sealing coats vs single-layered membranes; **b)** Comparison between different coloured sealing coats; **c)** Comparison between different coloured single-layered membranes; **d)** Comparison between different finished double-layered membranes.

Table 7
Differences in temperatures through the thickness of single-layered membranes, grouped in terms of structural aggregates.

Structural aggregates type	Weight [kg/m^2]	Thickness [mm]	$T_{SUP\ m}$ [°C]	$T_{BAS\ m}$ [°C]	ΔT [%]
Basalt	13.0	11.2	64.8	59.5	- 8.1
LECA	8.2	11.3	63.7	57.1	- 10.4
Limestone	12.3	11.0	64.0	59.4	- 7.1
Pale limestone	12.7	11.7	64.2	59.2	- 7.9

temperature reduction of 11.2 °C, 12.4 °C, 14.9 °C and 37.2 °C for Basalt, LECA, Limestone and Pale limestone, respectively, compared with the common bitumen sealing coat (Fig. 14**d**).

It is worth to specify that heat transfer through the membrane may be influenced by a number of factors such as thermal capacity and thermal conductivity of materials, inner composition of aggregates, interconnectivity between particles and others, which were not aimed to be considered in this study and that need further investigations.

Results from the comparison of average percentage temperature variation between T_{SUP} and T_{BAS} of single-layered membranes with the same binder finishing and different structural aggregates type are reported in Table 7.

Due their similar lithic composition, natural aggregates showed a slightly different thermal gradient through the thickness of membrane. On the contrary, membranes produced with LECA presented a more effective temperature reduction, probably due its porous inner composition. However, the monogranular configuration might not be appropriate to emphasize thermal-insulation properties of LECA, well know and investigated in other civil engineering applications. Nevertheless, its high-porosity guaranteed a general weight reduction of the membrane close to 40 %, if compared with basalt, which can be a remarkable design factor, in particular on steep dams.

5. Conclusions and further research

The aim of this study was to investigate the effectiveness of different sealing surface treatments for asphalt dams in terms of screening to solar radiation. Traditional and innovative techniques were tested, making use of conventional and alternative materials. Based on the results obtained, the following main conclusions can be drawn:

- Results of colorimetry analysis proved the effectiveness of binder pigmentation as an approach for landscaping mitigation of engineered constructions in non-urban scenarios. In this regard, due its clayey origin, LECA has been found as a more efficient solution when compared with natural aggregates finishing in double-layered membrane configurations;
- The use of multi-layered sealing treatments has been proved as a valid solution in reducing the asphalt layered system temperature, when compared with common sealing coats. The ultra-thin application, which makes use of the lowest quantity of materials, successfully achieved a temperature reduction up to 19 °C on average on the surface of standard impervious layers;
- The use of high-content calcium carbonate aggregates in the double-layered configuration led to a Steady-State Temperature of the sample of 41.6 °C, which was 15 % above the testing air temperature, resulting as the most efficient solution among the tested ones. It can be reasonably assumed that temperatures achieved using pale limestone as finishing aggregates, along with those obtained with other proposed solutions, may be adequate from a rheological standpoint to prevent blistering and slippage failures inside the asphalt layered system and into slowing thermal ageing processes on binders;
- All pigmented binders have been found more effective than black bitumen coatings in solar radiation screening, confirming the effectiveness of using high-reflective surfacing treatments to lower the temperature of asphalt layers. Among these, green-hued binders resulted a valid option that can also include visual impact mitigation in natural scenarios, due their high reflectivity in the IR region of the solar spectrum.

On one hand, this study attested the effectiveness of multi-functional surface treatments into decreasing the thermal burden on the structural impervious layers of asphalt, meeting the aims of the investigation. On the other hand, further research is needed to assess the consistency of this technology in time and to study the evolution of the screening properties of the proposed membranes. Since its recent development, this technique necessitates an adequate monitoring in in-situ applications, to determine its durability and its maintenance requirements. Furthermore, long-term ageing process needs further investigations. In this regard, the evaluation of the photo-oxidation effects of UV light on the sealing treatments is already in underway, and it will be discussed in future works.

CRediT authorship contribution statement

Piergiorgio Tataranni: Writing – review & editing, Supervision. **Filippo Balzano:** Writing – original draft, Methodology, Formal analysis, Data curation, Conceptualization. **Cesare Sangiorgi:** Writing – review & editing, Validation, Supervision. **Enrico Tita:** Writing – review & editing, Supervision, Resources.

Declaration of Competing Interest

The authors declare that they have no known competing financial interests or personal relationships that could have appeared to influence the work reported in this paper.

Data Availability

Data will be made available on request.

References

[1] T.G. Mezger, M.R. Rochlani. Bitumen Rheology, 1st ed., Anton Paar GmbH, Graz, Austria, 2023.
[2] I. Menzies, 1988, Waterproofing with asphalt. Water and Waste Treatment, vol. 31.
[3] K. Hrapović, Asphalt in hydraulic engineering, Eur. J. Sci. Innov. Technol. 2 (2) (2022) 130–146.
[4] Y. Zhang, W. Wang, Y. Zhu, Investigation on conditions of hydraulic fracturing for asphalt concrete used as impervious core in dams, Constr. Build. Mater. 93 (2015) 775–781, https://doi.org/10.1016/j.conbuildmat.2015.05.097.
[5] W. Wang, K. Höeg, The asphalt core embankment dam: a very competitive alternative, 1st Int. Symp. Rockfill Dams (2009) (Chengdu, China).
[6] C. Callari, P. Bertacchi, D. Cazzuffi, S. Di Maio, L. Sarti, and P. Sembenelli, "Embankment Dams with Bituminous Concrete Upstream Facing: Review and Recommendations - International Commission on Large Dams (ICOLD) Bulletin n. 114," 1999. [Online]. Available: ⟨https://www.researchgate.net/publication/347228515⟩.
[7] L. Kusari and F. Ahmedi, "Dams with impervious membrane of asphalt concrete," in BALWOIS 2008, Ohrid, Republic of Macedonia, 2008. [Online]. Available: ⟨https://www.researchgate.net/publication/242301449⟩.
[8] R.N. Hunter, et al.. The Shell Bitumen Handbook, sixth ed., ICE Publishing, London, 2015.
[9] R.B. Mallick, L. Jr. Allen Cooley, M.R. Teto, Ri.L. Bradbury, and D. Peabody, "An evaluation of factors affecting permeability of Superpave designed pavements," Auburn University, 2003.
[10] Z. Wang, J. Hao, Z. Sun, B. Ma, S. Xia, X. Li, Blistering mechanism analysis of hydraulic asphalt concrete facing, Appl. Sci. 9 (14) (2019), https://doi.org/10.3390/app9142903.
[11] L. Sarti, M. Kouris, O. Ierna, D. Cazzuffi, C. Villa, Waterproofing of earthfill dams with bituminous concrete facing the experience of Chabrouh dam (Lebanon) in summer 2007 (Ed.), *Rass. Del. Bitume N.° 57/07*, SITEB - Strade Ital. e bitumi (2007) 21–33.
[12] E. Schonian, The Shell Bitumen Hydraulic Engineering Handbook, ICE Publishing, London, 1999.

[13] S.N. Popchenko, Asphalt membranes for dams of local materials, Gidrotekhnicheskoe Stroit. 'stvo (11) (1969) 15–18.
[14] J. Cunning, A. Isidoro, T. Eldridge, J. Reinson, Dam construction at diavik using bituminous geomembrane liners, GeoEdmonton '08 - 61st Can. Geotech. Conf. (2008) (Edmonton, Canada).
[15] K. Adam, J. Říha, M. Špano, Investigation on the temperature of the asphalt-concrete facing of embankment dams, Int. J. Pavement Res. Technol. 9 (1) (2016) 73–81, https://doi.org/10.1016/j.ijprt.2016.01.006.
[16] A.C. Crawford, D.M. Kriech, L.A. Smith, L.V. Osborn, A.J. Kriech, Assessing the effects of sunlight and water on asphalt binder and pavement leachability related to the environment, J. Environ. Manag. 345 (2023), https://doi.org/10.1016/j.jenvman.2023.118638.
[17] Y. Sun, H. Li, B. Yang, Y. Han, Z. Zou, Investigation on rheological properties and aging mechanism of asphalt under multiple environmental conditions, Constr. Build. Mater. 443 (2024), https://doi.org/10.1016/j.conbuildmat.2024.137713.
[18] Z. He, T. Xie, H. Yu, J. Ge, W. Dai, Evaluation of quantum dot composite graphene /titanium oxide enhanced UV aging resistance modified asphalt, Constr. Build. Mater. 408 (2023), https://doi.org/10.1016/j.conbuildmat.2023.133732.
[19] H. Liu, Z. Zhang, Z. Tian, C. Lu, Exploration for UV aging characteristics of asphalt binders based on response surface methodology: insights from the UV aging influencing factors and their interactions, Constr. Build. Mater. 347 (2022), https://doi.org/10.1016/j.conbuildmat.2022.128460.
[20] N. Tran, B. Powell, Strategies for design and construction of high-reflectance asphalt pavements, Auburn, Al (2009).
[21] R.A. Page, D.M. Broore, and R.F. Yerkes, "The Los Angeles Dam Story: U.S. Geological Survey Fact Sheet 096–95," Los Angeles, 1995. Accessed: May 06, 2024. [Online]. Available: ⟨https://pubs.usgs.gov/fs/1995/0096/⟩.
[22] M. Wieland, Life-span of storage dams, Int. Water Power Mag. 62 (2010) 32–35.
[23] G. Cloete and S. Shaanika, "Asphalt resealing of the 35m high Von Bach Dam," in *AFRICA 2019: Water storage and Hydropower development for Africa*, Windhoek, Namibia, 2019. [Online]. Available: ⟨https://www.researchgate.net/publication/342410612⟩.
[24] DGGT - Deutsche Gesellschaft für Geotechnik, *Empfehlungen für die Ausführung von Asphaltarbeiten im Wasserbau*, 5th ed. Karlsruhe, 2008.
[25] M.Q.J. Mafra and T. Eldridge, "Two Case Histories of Dams Waterproofing with Bituminous Geomembrane," in *The First Pan American Geosynthetics Conference & Exhibition*, Cancun, Mexico, 2020. [Online]. Available: ⟨https://www.researchgate.net/publication/340514596⟩.
[26] G. Zhu, et al., Impact of landscape dams on river water cycle in urban and peri-urban areas in the Shiyang River Basin: Evidence obtained from hydrogen and oxygen isotopes, J. Hydrol. (Amst.) 602 (2021), https://doi.org/10.1016/j.jhydrol.2021.126779.
[27] B. Reed, An introduction to visual impact assessment, in: R. Shaw, T. Jackson (Eds.), Loughborough University, WEDC - Water Engineering and Development Centre, Leicestershire, UK, 2017.
[28] J. Hu, X. (Bill) Yu, Reflectance spectra of thermochromic asphalt binder: characterization and optical mixing model, J. Mater. Civ. Eng. 28 (2) (2016), https://doi.org/10.1061/(asce)mt.1943-5533.0001387.
[29] R.J. Cominsky, G.A. Huber, T.W. Kennedy, M. Anderson, The Superpave Mix Design Manual for New Construction and Overlays, Strategic Highway Research Program, Washington, DC, 1994.
[30] E.J. Yoder, M.W. Witzak. Principles of Pavement Design, 2nd ed., Wuley and Sons, New York,NY, 1975.
[31] E.M. Mohammed, H. Nebdi, M. El Malki, C. Hajjaj, H. Nebdi1, Theoretical modeling of variation in solar irradiance outside the Earth atmosphere, Int. J. Tech. Phys. Probl. Eng. 16 (58) (2024) 374–384. ⟨www.iotpe.com⟩ ([Online]. Available:).
[32] K. Stamnes, Ultraviolet radiation, in: J.R. Holton (Ed.), Encycl. Atmos. Sci. (2002) 2467–2473.
[33] I. Kousis, C. Fabiani, L. Ercolanoni, A.L. Pisello, Using bio-oils for improving environmental performance of an advanced resinous binder for pavement applications with heat and noise island mitigation potential, Sustain. Energy Technol. Assess. 39 (2020), https://doi.org/10.1016/j.seta.2020.100706.
[34] L. Wang, J. Yu, Principles of photocatalysis, in: in *S-scheme Heterojunction Photocatalysts*, 35, Interface Science and Technology, 2023, pp. 1–52, https://doi.org/10.1016/B978-0-443-18786-5.00002-0.
[35] V.R. Serdyuk, Investigation of changes in high temperature performance of asphalt concrete under ultraviolet radiation, Mod. Technol. Methods Calc. Constr. 20 (2024) 127–134, https://doi.org/10.36910/6775-2410-6208-2023-10(20)-14.
[36] B. Li, Y. Wang, X. Ren, X. Teng, X. Su, Influence of ultraviolet aging on adhesion performance of warm mix asphalt based on the surface free energy theory, Appl. Sci. (Switz.) 9 (10) (2019), https://doi.org/10.3390/app9102046.
[37] M. Van De Ven, A. Molenaar, E. Hagos, Influence of UV on laboratory ageing of porous asphalt concrete compared to field ageing, 11th Int. Conf. Asph. Pavements (2010) (Nagoya, Japan).
[38] J. Meseguer, I. Pérez-Grande, and A. Sanz-Andrés, *Spacecraft thermal control*. Cambridge, 2012.
[39] R.R. Baniya, "Study of various metrics evaluating color quality of light sources," Master of Science, Aalto University, Espoo, 2012. [Online]. Available: ⟨https://www.researchgate.net/publication/283213366⟩.
[40] O. Lima, et al., Mitigation of urban heat island effects by thermochromic asphalt pavement, Coatings 13 (1) (2023), https://doi.org/10.3390/coatings13010035.
[41] I.H. Akbari, R. Levinson, P. Berdahl, ATSM Standards for measuring solar reflectance and infrared emittance of construction materials and comparing their steady-state surface temperatures. American Council for an Energy Efficient Economy Summer Study, Ernest Orlando Lawrence Berkeley National Laboratory, Ed., Pacific Grove, CA, 1996.
[42] P. Berdahl, S.E. Bretz, Preliminary survey of the solar reflectance of cool roofing materials, Energy Build. 25 (1997) 149–158.
[43] K. Dornelles, V.F. Roriz, M. Roriz, V. Roriz, M. Roriz, Determination of the solar absorptance of opaque surfaces, PLEA2007 - 24th Conf. Passiv. Low. Energy Archit. (2007), https://doi.org/10.13140/RG.2.1.2368.1764.
[44] NASA), "Reflected Near-Infrared Waves," Science Mission Directorate. Accessed: Jun. 03, 2024. [Online]. Available: ⟨http://science.nasa.gov/ems/08_nearinfraredwaves⟩.
[45] ATLAS - Weatheting Testing Solutions, Weathering Testing Guidebook. 2001.
[46] Y.K. Shrestha, S.K. Shrestha, Fundamentals of colorimetry, in: K. Samanta (Ed.), Advances in colorimetry, A, IntechOpen, 2023. ⟨www.intechopen.com⟩ ([Online]. Available).
[47] Commission International de l'Eclairage, "CIE Division 1: Vision and color," in Minutes of the 3rd Meeting of the Luo Terms, Princeton, New Jersey, USA, Jun. 2010.
[48] Y.-F. Chou, M.R. Luo, J. Schanda, P. Csuti, F. Szabo, G. Sárvári, Recent Developments in Colour Rendering Indices and Their Impacts in Viewing Graphic Printed Materials, Color Imaging Conf. 19 (1) (Jan. 2011) 61–65, https://doi.org/10.2352/CIC.2011.19.1.art00014.
[49] B. Fraser, C. Murphy, F. Bunting. Real world color management, 2nd ed., Peachpit Press, Berkley (CA), 2005.
[50] M.D. Fairchild. Color Appearance Models, 2nd ed., John Wiley & Sons, Ltd, 2006.
[51] Z. Fan, et al., Measurement of Soil Color: A Comparison Between Smartphone Camera and the Munsell Color Charts, Soil Sci. Soc. Am. J. 81 (5) (Sep. 2017) 1139–1146, https://doi.org/10.2136/sssaj2017.01.0009.
[52] B. De Pascale, P. Tataranni, C. Lantieri, A. Bonoli, C. Sangiorgi, Innovative light-coloured porous asphalt for low-impact pavements: A laboratory investigation, Constr. Build. Mater. 368 (Mar. 2023), https://doi.org/10.1016/j.conbuildmat.2023.130482.
[53] P. Tataranni, G.M. Besemer, V. Bortolotti, C. Sangiorgi, Preliminary research on the physical and mechanical properties of alternative lightweight aggregates produced by alkali-activation ofwaste powders, Materials 10 (7) (Jul. 2018), https://doi.org/10.3390/ma11071255.
[54] S. Copetti Callai, P. Tataranni, M. De Rose, A. Natali Murri, R. Vaiana, C. Sangiorgi, A Preliminary Laboratory Evaluation of Artificial Aggregates from Alkali-Activated Basalt Powder, Sustain. (Switz.) 14 (24) (Dec. 2022), https://doi.org/10.3390/su142416653.
[55] B. Ayati, V. Ferrándiz-Mas, D. Newport, and C. Cheeseman, "Use of clay in the manufacture of lightweight aggregate," Feb. 20, 2018, Elsevier Ltd. doi: 10.1016/j.conbuildmat.2017.12.018.
[56] ISO 9845-1, *Solar energy - Reference solar spectral irradiance at the ground at different receiving conditions | Part 1: Direct normal and hemispherical solar irradiance for air mass 1,5*. 2022.

[57] F. Praticò, M. Giunta, and C. Marino, "Pavement albedo and sustainability: An experimental investigation," Aug. 2012. [Online]. Available: ⟨https://www.researchgate.net/publication/284726139⟩.
[58] I. Cambridge Systematics, "Cool Pavement Report: EPA Cool Pavements Study - Task 5," Washington, DC, 2005. [Online]. Available: ⟨www.camsys.com⟩.
[59] H. Li, J.T. Harvey, T.J. Holland, and M. Kayhanian, "The use of reflective and permeable pavements as a potential practice for heat island mitigation and stormwater management," 2013, Institute of Physics Publishing. doi: 10.1088/1748-9326/8/4/049501.
[60] A. Synnefa, T. Karlessi, N. Gaitani, M. Santamouris, D.N. Assimakopoulos, C. Papakatsikas, Experimental testing of cool colored thin layer asphalt and estimation of its potential to improve the urban microclimate, Build. Environ. 46 (1) (Jan. 2011) 38–44, https://doi.org/10.1016/j.buildenv.2010.06.014.
[61] Munsell Color Company, Munsell Soil Color Charts, 2009rev ed., Munsell Color Company, Baltimore, 1975.
[62] D. Hammonds, Soil colors and their interpretation. in *Division of Disease Control and Healt Protection*, Florida Department of Healt, Apr. 2015.
[63] Munsell Color Company, Munsell Color Charts for plant tissues, 2nd, rev ed. Baltimore, 1977.
[64] K. Tanaka, Y. Kato, A. Mizuno, M. Mikawa, M. Fujisawa, Dynamic grass color scale display technique based on grass length for green landscape-friendly animation display, Sci. Rep. 13 (1) (Dec. 2023), https://doi.org/10.1038/s41598-022-27183-x.
[65] A. Synnefa, M. Santamouris, K. Apostolakis, On the development, optical properties and thermal performance of cool colored coatings for the urban environment, Sol. Energy 81 (4) (Apr. 2007) 488–497, https://doi.org/10.1016/j.solener.2006.08.005.
[66] I. Kousis, C. Fabiani, A.L. Pisello, Could a bio-resin and transparent pavement improve the urban environment? An in field thermo-optical investigation and life-cycle assessment, Sustain Cities Soc. 79 (Apr. 2022), https://doi.org/10.1016/j.scs.2021.103597.
[67] A. Kume, T. Akitsu, K.N. Nasahara, Leaf color is fine-tuned on the solar spectra to avoid strand direct solar radiation, J. Plant Res 129 (4) (Jul. 2016) 615–624, https://doi.org/10.1007/s10265-016-0809-0.
[68] T.W. Tibbits, "International Lighting in Controlled Environments Workshop," in NASA-CP-95-3309, Kennedy Space Center, Florida: National Aeronautics and Space Administration (NASA), Mar. 1994.
[69] G. Badin, Y. Huang, N. Ahmad, Comparative Analysis of Thermally Investigated Pigment-Modified Asphalt Binders, Airfield Highw. Pavements (2023) 174–184.